# Prediction and Optimization of Weld Bead Volume for the Submerged Arc Process — Part 1

*The main and interaction effects of the process-control variables on important bead geometry parameters were determined quantitatively and are presented graphically*

BY V. GUNARAJ AND N. MURUGAN

ABSTRACT. Because of its high quality and reliability, submerged arc welding (SAW) is one of the chief metal-joining processes employed in industry for the manufacture of steel pipes used for various applications. This paper highlights a study and analysis of various process-control variables and important weld bead quality parameters in SAW of pipes manufactured out of structural steel (IS: 2062). Mathematical models were developed for the submerged arc welding of 6-mm-thick structural steel plates using 3.15-mm-diameter steel electrodes.

The models were developed using the five-level factorial technique to relate the important process-control variables — welding voltage, wire feed rate, welding speed and nozzle-to-plate distance — to a few important bead-quality parameters — penetration, reinforcement, bead width, total volume of the weld bead and dilution. The models developed were checked for their adequacy with the F test. Using the models, the main and interaction effects of the process-control variables on important bead geometry parameters were determined quantitatively and presented graphically.

The developed models and the graphs showing the direct and interaction effects of process variables on the bead geometry are very useful in selecting the process parameters to achieve the desired weld-bead quality. Also, the precision of the results obtained with the mathematical models were tested by using conformity test runs. The test runs were conducted nearly two years after the development of mathematical models with the same experimental setup, and it was found the accuracy of the predicted results is about 98%. Further, these mathematical models help to optimize SAW to make it a more cost-effective process.

*V. GUNARAJ is Assistant Professor of Mechanical Engineering, Kumaraguru College of Technology, Coimbatore, Tamil Nadu, India. N. MURUGAN is Assistant Professor of Mechanical Engineering, Coimbatore Institute of Technology, Coimbatore, Tamil Nadu, India.*

## Introduction

Submerged arc welding is one of the major fabrication processes in industry because of its inherent advantages, including deep penetration and a smooth bead (Refs.1, 2). In the SAW of pipes, engineers often face the problem of selecting appropriate and optimum combinations of input process-control variables for achieving the required weld bead quality or predicting the weld bead quality for the proposed process-control-variable values (Ref. 3). For automatic SAW, the control parameters must be fed to the system according to some mathematical formula to achieve the desired results (Ref. 4). These important problems can be solved with the development of mathematical models through effective and strategic planning, design and execution of experiments.

To achieve this, statistically designed experiments based on the factorial technique were used to reduce the cost and time, as well as to obtain the required information about the main and the interaction effects on the response parameters (Refs. 5, 6). A cross section of a weld bead showing the important weld bead quality parameters is given in Fig. 1.

The mathematical models developed are useful for selecting correct process parameters to achieve the desired weld bead quality and to predict weld bead quality for the given process parameters (Ref. 7). These models facilitate optimization of the process and sensitivity analysis. They also help to improve the understanding of the effect of process parameters on bead quality, to evaluate the interaction effects of bead parameters and to optimize the bead quality to obtain a high-quality welded joint at a relatively low cost with high productivity.

**KEY WORDS**

Dilution
SAW
Optimization
Bead Geometry
Weld Bead Penetration
Weld Bead Reinforcement
Weld Bead Width
Design Matrix

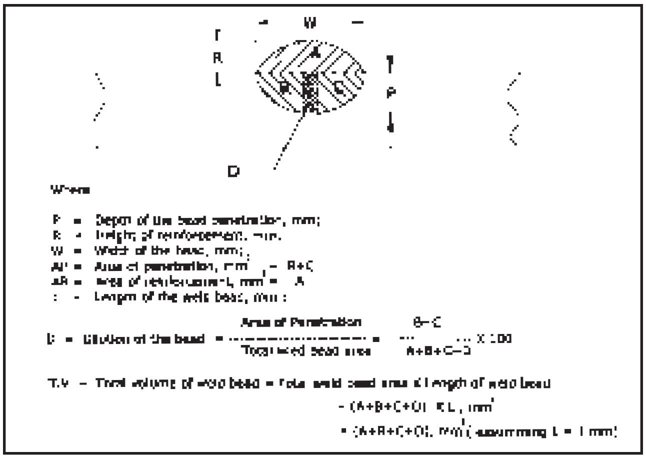


Fig. 1 — Cross section of a weld bead.

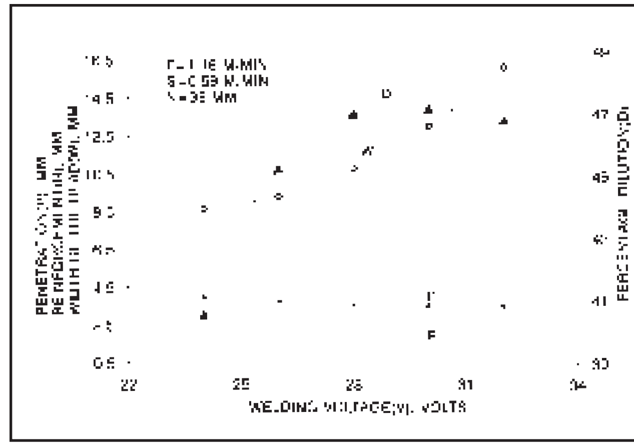


Fig. 2 — Direct effect of welding voltage (V) on bead parameters (P, R, W, D).

## Experimental Procedure

The experiment was conducted at M/s. Sri Venkateswara Engineering Corp., Coimbatore, India, with the following setup.

ADORE semiautomatic welding equipment with a constant-voltage, rectifier-type power source with a 1200-A capacity was used to join IS: 2062, structural steel plates 300 x 150 x 6 mm. ESAB SA1 (E8), 3.15-mm-diameter, copper-coated electrode in coil form and ESAB-brand, basic-fluoride-type (equivalent to DIN 8557) granular flux was used. A square butt joint with a 1-mm root opening was selected to join the plates in the flat position, keeping the electrode positive and perpendicular to the plate.

## Plan of Investigation

The research work was carried out in the following steps (Ref. 8).

- Identifying the important process-control variables.
- Finding the upper and lower limits of the control variables.
- Developing the design matrix.
- Conducting the experiments as per the design matrix.
- Recording the responses.
- Developing the mathematical models.
- Calculating the coefficients of the polynomials.
- Checking the adequacy of the models developed.
- Arriving at the final mathematical models.
- Conducting the conformity test.
- Presenting the direct and interaction effects of different process parameters on bead geometry graphically.
- Analyzing the results.

**Table 1 — Process Control Parameters and Their Limits**

| Parameters | Units | Notation | Limits –2 | –1 | 0 | +1 | +2 |
|---|---|---|---|---|---|---|---|
| Welding voltage | volts | V | 24 | 26 | 28 | 30 | 32 |
| Wire feed rate | m/min. | F | 0.70 | 0.93 | 1.16 | 1.39 | 1.62 |
| Welding speed | m/min. | S | 0.43 | 0.51 | 0.59 | 0.67 | 0.75 |
| Nozzle-to-plate distance | mm | N | 30.00 | 32.50 | 35.0 | 37.5 | 40.0 |

## Identification of the Process Variables

The independently controllable process parameters affecting bead geometry and the quality of the weld bead were open-circuit voltage (OCV), wire feed rate (F), welding speed (S) and nozzle-to-plate distance (N). As it was not possible to control the welding voltage (V) directly in the power source used for conducting the experiments, OCV was used as a process variable. However, V was correlated to OCV through the development of a mathematical model. Using the developed model, welding voltage (V) was calculated for all values of OCV and treated as a factor for drawing graphs and analyzing results.

### Finding the Limits of the Process Variables

Trial runs were carried out by varying one of the process parameters while keeping the rest of them at constant values (Ref. 9). The working range was decided upon by inspecting the bead for a smooth appearance without any visible defects such as surface porosity and undercut. The upper limit of a factor was coded as +2 and the lower limit as –2. The coded values for intermediate values were calculated from the following relationship: $X_i = 2[2X - (X_{max} + X_{min})] / (X_{max} – X_{min})$, where $X_i$ is the required coded value of a variable X; X is any value of the variable from $X_{min}$ to $X_{max}$; $X_{min}$ is the lower level of the variable and $X_{max}$ is the upper level of the variable. The process-variable levels with their units and notations are given in Table 1.

### Developing the Design Matrix

The selected design matrix, shown in Table 2, is a five-level, four-factor, central composite rotatable factorial design (Ref. 10) consisting of 31 sets of coded conditions. It comprises a full replication of $2^4$ (=16) factorial design plus seven center points and eight star points. All welding variables at their intermediate level (0) constitute the center points, and the combinations of each of the welding variables at either its lowest (–2) or highest (+2) with the other three variables at their intermediate level constitute the star points. Thus, the 31 experimental runs allowed the estimation of the linear, quadratic and two-way interactive ef-

**Table 2 — Design Matrix and Observed Values of Bead Parameters**

| | Design Matrix | | | | Weld Bead Parameters | | | | | | |
|---|---|---|---|---|---|---|---|---|---|---|---|
| S. No. | V | F | S | N | P mm | R mm | W mm | AP ($mm^2$) | AR ($mm^2$) | D (%) | T.V ($mm^3$) |
| 1 | –1 | –1 | –1 | –1 | 3.52 | 1.70 | 10.15 | 20.7 | 24.48 | 42.40 | 48.8 |
| 2 | +1 | –1 | –1 | –1 | 3.40 | 1.51 | 13.47 | 22.1 | 21.52 | 46.80 | 47.3 |
| 3 | –1 | +1 | –1 | –1 | 4.75 | 2.32 | 11.05 | 24.5 | 22.80 | 47.50 | 51.5 |
| 4 | +1 | +1 | –1 | –1 | 4.10 | 1.85 | 15.64 | 26.3 | 24.15 | 50.30 | 52.2 |
| 5 | –1 | –1 | +1 | –1 | 3.25 | 1.38 | 08.28 | 18.3 | 23.17 | 40.70 | 44.9 |
| 6 | +1 | –1 | +1 | –1 | 3.18 | 1.18 | 10.10 | 19.5 | 23.42 | 41.90 | 46.5 |
| 7 | –1 | +1 | +1 | –1 | 3.52 | 1.50 | 09.15 | 21.5 | 18.90 | 48.60 | 44.3 |
| 8 | +1 | +1 | +1 | –1 | 3.33 | 1.82 | 09.86 | 23.2 | 19.25 | 49.80 | 46.6 |
| 9 | –1 | –1 | –1 | +1 | 3.85 | 1.61 | 10.66 | 20.2 | 27.48 | 39.40 | 51.3 |
| 10 | +1 | –1 | –1 | +1 | 3.60 | 1.48 | 14.55 | 21.8 | 26.24 | 40.50 | 53.8 |
| 11 | –1 | +1 | –1 | +1 | 4.10 | 1.92 | 13.38 | 23.1 | 27.82 | 42.10 | 54.9 |
| 12 | +1 | +1 | –1 | +1 | 3.80 | 1.80 | 15.96 | 26.5 | 31.16 | 42.90 | 61.8 |
| 13 | –1 | –1 | +1 | +1 | 3.20 | 1.37 | 08.70 | 17.7 | 24.52 | 38.60 | 45.5 |
| 14 | +1 | –1 | +1 | +1 | 3.00 | 1.10 | 09.28 | 18.9 | 25.34 | 39.70 | 47.6 |
| 15 | –1 | +1 | +1 | +1 | 4.10 | 1.75 | 09.01 | 20.3 | 25.55 | 40.80 | 49.8 |
| 16 | +1 | +1 | +1 | +1 | 3.88 | 1.50 | 10.00 | 21.1 | 23.87 | 42.30 | 49.1 |
| 17 | –2 | 0 | 0 | 0 | 4.10 | 1.62 | 10.28 | 19.4 | 24.25 | 41.10 | 47.2 |
| 18 | +2 | 0 | 0 | 0 | 3.75 | 1.43 | 15.30 | 25.4 | 29.45 | 42.90 | 59.2 |
| 19 | 0 | –2 | 0 | 0 | 3.26 | 1.41 | 09.95 | 19.1 | 17.95 | 38.10 | 40.1 |
| 20 | 0 | +2 | 0 | 0 | 4.97 | 1.75 | 10.96 | 27.7 | 21.53 | 51.00 | 54.3 |
| 21 | 0 | 0 | –2 | 0 | 4.25 | 2.30 | 16.11 | 25.3 | 31.33 | 41.30 | 61.2 |
| 22 | 0 | 0 | +2 | 0 | 3.48 | 1.40 | 08.50 | 18.4 | 21.05 | 43.00 | 42.8 |
| 23 | 0 | 0 | 0 | –2 | 3.82 | 1.31 | 11.17 | 22.5 | 19.68 | 48.70 | 46.2 |
| 24 | 0 | 0 | 0 | +2 | 3.58 | 1.27 | 12.05 | 23.2 | 27.83 | 42.50 | 54.6 |
| 25 | 0 | 0 | 0 | 0 | 3.45 | 1.15 | 11.20 | 20.9 | 21.80 | 47.10 | 44.4 |
| 26 | 0 | 0 | 0 | 0 | 3.47 | 1.30 | 10.58 | 21.7 | 21.40 | 46.50 | 46.6 |
| 27 | 0 | 0 | 0 | 0 | 3.66 | 1.27 | 09.92 | 21.9 | 19.80 | 48.20 | 45.4 |
| 28 | 0 | 0 | 0 | 0 | 3.60 | 1.31 | 11.13 | 21.2 | 19.90 | 47.60 | 44.5 |
| 29 | 0 | 0 | 0 | 0 | 3.30 | 1.16 | 10.56 | 20.5 | 21.10 | 45.70 | 44.9 |
| 30 | 0 | 0 | 0 | 0 | 3.60 | 1.27 | 10.84 | 22.6 | 21.50 | 47.30 | 47.8 |
| 31 | 0 | 0 | 0 | 0 | 3.92 | 1.45 | 11.05 | 22.1 | 24.60 | 48.50 | 47.6 |

fects of the welding variables on the bead geometry.

### Conducting the Experiments as Per the Design Matrix

The experiments were conducted as per the design matrix at random to avoid systematic errors infiltrating the system. Beads were laid on the joint to join 6-mm-thick structural steel plates with the experimental setup explained previously.

### Recording the Responses

The welded plates were cut at the center of the bead to obtain 10-mm-wide test specimens. These specimens were prepared by the usual metallurgical polishing methods and etched with 2% nital. The weld bead profiles were traced using a reflective-type optical profile projector with 10X magnification. The bead dimensions — namely, penetration (P), width (W) and reinforcement (R) — were measured with a digital planimeter with 1-µm accuracy. The areas of the base plate melted and the excess metal deposited over the base metal — namely, area of penetration (AP) and area of reinforcement (AR), respectively — were also measured using the planimeter. The percentage of dilution (D) and the total area of the weld bead were calculated. The total volume (T.V) of the weld bead, assuming the length of the bead (L) as unity, was also calculated. The observed and calculated values are given in Table 2.

### Development of Mathematical Models

The response function representing any of the weld bead dimensions can be expressed as y = f (V, F, S, N). The relationship selected, being a second-degree response surface, is expressed as follows (Ref. 11):

$$Y = b_0 + b_1V + b_2F + b_3S + b_4N + b_{11}V^2 + b_{22}F^2 + b_{33}S^2 + b_{44}N^2 + b_{12}VF + b_{13}VS + b_{14}VN + b_{23}FS + b_{24}FN + b_{34}SN.$$

### Evaluation of the Coefficients of Models

The values of the coefficients were calculated by regression analysis with the help of the following equations (Ref. 12):

$$b_n = 0.142857 \quad Y - 0.035714 \quad (X_{ii}Y)$$

$$b_i = 0.041667 \quad (X_iY)$$

$$b_{ii} = 0.03125 \quad (X_{ii}Y) - 0.035714 \quad (X_{ii}Y) - 0.035714 \quad Y$$

$$b_{ij} = 0.0625 \quad (X_{ij}Y)$$

A computer program was developed to calculate the value of these coefficients for different responses. The calculated values are presented in Table 3.

### Checking the Adequacy of the Developed Models

The adequacy of the models was then tested by the analysis-of-variance technique (ANOVA) (Ref. 13). The calculated value of the F ratio of the model developed does not exceed the tabulated value of F ratio for a desired level of confidence (selected as 95%). If the calculated value of the R ratio of the model developed exceeds the standard tabulated value of the R ratio for a desired level of confidence (95%), then the models are adequate (Ref. 14). From Table 4, it is evident that, for all the models, the above conditions are satisfied and, hence, adequate.

### Development of Final Mathematical Models

The final mathematical models developed are given below. The process-control variables are in their coded form.

$$\text{Penetration, mm} = 3.57 - 0.113V + 0.33F - 0.217S - 0.001N + 0.048V^2 + 0.1F^2 + 0.03S^2 - 0.01N^2 - 0.05VF + 0.06VS + 0.04VN - 0.01FS - 0.01FN + 0.08SN \quad (1)$$

Table 3 — Regression Coefficients of Models

| SL. No. | Coefficient | P mm | R mm | W mm | AP $(mm^2)$ | AR $(mm^2)$ | D (%) | T.V $(mm^3)$ |
|---|---|---|---|---|---|---|---|---|
| | | Bead Parameters | | | | | | |
| 1 | $b_0$ | 3.572 | 1.27 | 10.76 | 21.56 | 21.44 | 47.27 | 45.78 |
| 2 | $b_1$ | –0.113 | –0.08 | 1.19 | 1.05 | 0.443 | 0.74 | 1.58 |
| 3 | $b_2$ | 0.33 | 0.16 | 0.45 | 1.85 | 0.187 | 2.50 | 2.20 |
| 4 | $b_3$ | –0.217 | –0.18 | –1.90 | –1.61 | –1.76 | 0.25 | –3.50 |
| 5 | $b_4$ | –0.001 | –0.03 | 0.23 | –0.21 | 2.11 | –2.23 | 2.00 |
| 6 | $b_{11}$ | 0.05 | 0.07 | 0.41 | 0.04 | 1.39 | 1.31 | 1.67 |
| 7 | $b_{22}$ | 0.10 | 0.08 | –0.17 | 0.29 | –0.39 | –0.71 | 0.17 |
| 8 | $b_{33}$ | 0.03 | 0.15 | 0.29 | –0.097 | 1.22 | –1.31 | 1.34 |
| 9 | $b_{44}$ | –0.01 | 0.01 | 0.12 | 0.15 | 0.62 | –0.44 | 0.97 |
| 10 | $b_{12}$ | –0.05 | 0.02 | –0.05 | 0.14 | 0.41 | –0.09 | 0.28 |
| 11 | $b_{13}$ | 0.06 | 0.03 | –0.64 | –0.21 | –0.047 | –0.28 | –0.21 |
| 12 | $b_{14}$ | 0.038 | –0.014 | –0.15 | 0.056 | 0.14 | –0.31 | 0.48 |
| 13 | $b_{23}$ | –0.011 | –0.003 | –0.35 | –0.24 | –0.94 | 0.43 | –0.87 |
| 14 | $b_{24}$ | –0.01 | –0.02 | 0.09 | –0.16 | 0.77 | –0.90 | 0.64 |
| 15 | $b_{34}$ | 0.083 | 0.03 | –0.29 | –0.16 | –0.33 | 0.17 | –0.77 |

Reinforcement, mm = $1.27 - 0.08V + 0.16F - 0.18S - 0.03N + 0.07V^2 + 0.078^2 + 0.15S^2 + 0.01N^2 + 0.03VF + 0.03VS - 0.014VN - 0.003FS - 0.02FN + 0.03SN$ (2)

Width of weld bead, mm = $10.76 + 1.19V + 0.45F - 1.9S + 0.23N + 0.41V^2 - 0.17F^2 + 0.29S^2 + 0.12N^2 - 0.04VF - 0.64VS - 0.15VN - 0.35FS + 0.091FN - 0.29SN$ (3)

Area of penetration, $mm^2$ = $21.56 + 1.05V + 1.85F - 1.61S - 0.212N + 0.041V^2 + 0.29F^2 - 0.097S^2 + 0.15N^2 + 0.14VF - 0.21VS + 0.056VN - 0.24FS - 0.16FN - 0.16SN$ (4)

Area of reinforcement, $mm^2$ = $21.44 + 0.44V + 0.187F - 1.76S + 2.11N + 1.39V^2 - 0.39F^2 + 1.22S^2 + 0.62N^2 + 0.41VF - 0.047VS + 0.14VN - 0.94FS + 0.77FN - 0.33SN$ (5)

Percentage of dilution = $47.27 + 0.74V + 2.51F - 0.25S - 2.23N - 1.31V^2 - 0.71F^2 - 1.31S^2 - 0.44N^2 - 0.09VF - 0.3VS - 0.31VN + 0.43FS - 0.90FN + 0.17SN$ (6)

Total weld bead volume, $mm^3$ = $45.78 + 1.58V + 2.2F - 3.5S + 2.0N + 1.67V^2 + 0.17F^2 + 1.34S^2 + 0.97N^2 + 0.28VF - 0.21VS + 0.48VN - 0.87FS + 0.64FN - 0.77SN$ (7)

The significance of the coefficients were also tested using the SYSTAT software package (Ref.15), and the reduced models with significant coefficients were developed. It was found the reduced models were better than the full models because the reduced models have higher values of $R^2$ (adjusted) and lesser values of standard-error estimates than that of the full models. The values of $R^2$ and standard error of estimates for both the models are given in Table 5. The final reduced mathematical models with the significant coefficients are given below:

Penetration, mm = $3.64 - 0.113V + 0.33F - 0.217S + 0.05V^2 + 0.1F^2 + 0.03S^2$ (8)

Reinforcement, mm = $1.29 - 0.08V + 0.16F - 0.18S + 0.07V^2 + 0.08F^2 + 0.15S^2$ (9)

Width of weld bead, mm = $10.87 + 1.19V + 0.45F - 1.9S + 0.23N + 0.4V^2 - 0.19F^2 + 0.28S^2 - 0.64VS - 0.35FS - 0.29SN$ (10)

Area of penetration, $mm^2$ = $21.64 + 1.05V + 1.85F - 1.6S + 0.29F^2$ (11)

Area of reinforcement, $mm^2$ = 21.05 +

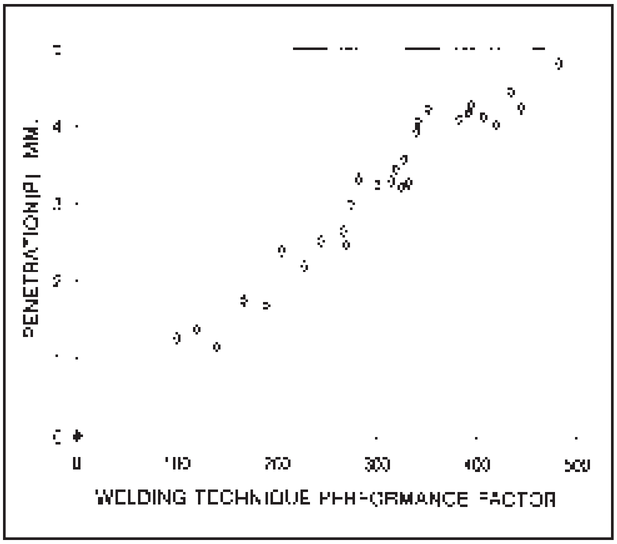

Fig. 3 — Effect of the welding performance factor on penetration.

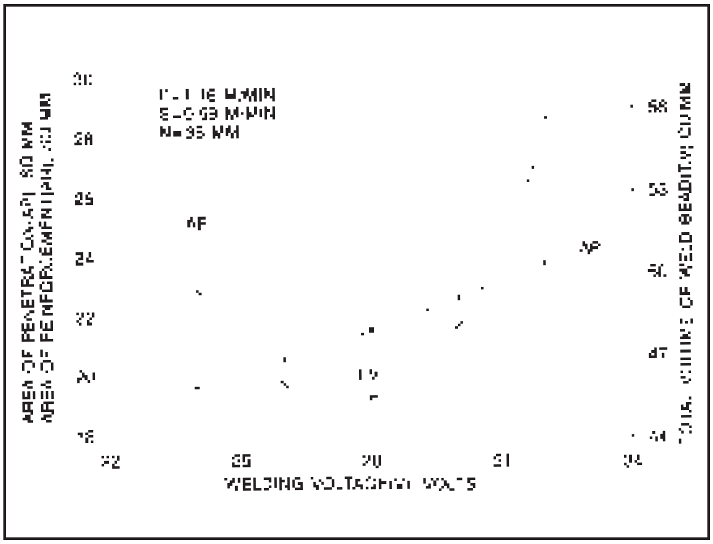

Fig. 4 — Direct effect of welding voltage (V) on bead parameters (AP, AR and T.V).

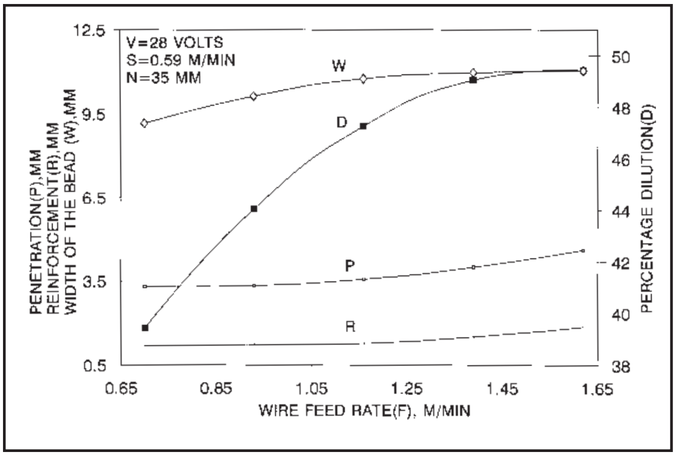


*Fig. 5 — Direct effect of wire feed rate (F) on bead parameters P, R, W and D.*

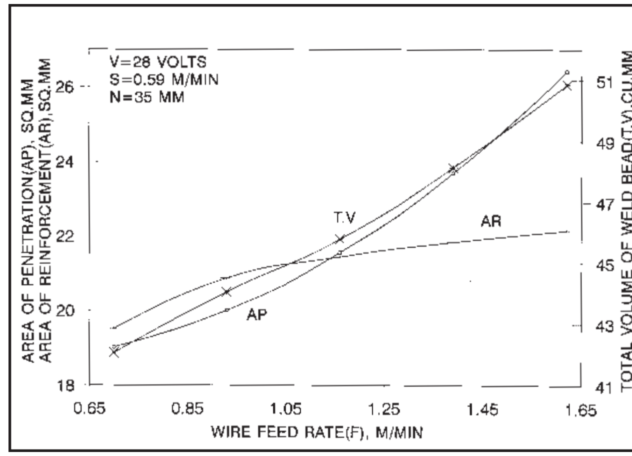


*Fig. 6 — Direct effect of wire feed rate (F) on bead parameters AP, AR and T.V.*

**Table 4 — Calculation of Variants for Testing the Adequacy of the Models**

| | First order terms | | Second order terms | | Lack of fit | | Error-terms | | | | |
|---|---|---|---|---|---|---|---|---|---|---|---|
| Bead Parameters | S.S | D.F | S.S | D.F | S.S | D.F | S.S | D.F | F-ratio | R-ratio | Whether model is adequate |
| Penetration | 4.10 | 4 | 0.50 | 10 | 1.03 | 10 | 0.23 | 6 | 2.68 | 8.58 | Adequate |
| Reinforcement | 1.55 | 4 | 0.92 | 10 | 0.27 | 10 | 0.06 | 6 | 2.70 | 17.29 | Adequate |
| Bead width | 127.2 | 4 | 18.80 | 10 | 3.57 | 10 | 1.20 | 6 | 1.79 | 52.18 | Adequate |
| Area of Penetration | 171.6 | 4 | 6.22 | 10 | 12.3 | 10 | 3.18 | 6 | 2.31 | 23.84 | Adequate |
| Area of reinforcement | 186.4 | 4 | 134.1 | 10 | 34.4 | 10 | 15.3 | 6 | 1.35 | 8.98 | Adequate |
| Bead dilution | 287.1 | 4 | 117.4 | 10 | 24.9 | 10 | 5.60 | 6 | 2.68 | 31.10 | Adequate |
| Total weld bead volume | 569.2 | 4 | 168.9 | 10 | 82.6 | 10 | 12.45 | 6 | 3.98 | 25.41 | Adequate |

R-ratio = 3.96 = (Sum of squares of first and second order terms/ Sum of D.F of first and second order terms)/M.S of error terms.
F-ratio $_{(10,6,0.05)}$ = 4.09 = M.S of Lack of fit/M.S of error terms.
S.S = Sum of squares; D.F = Degree of freedom; M.S = Mean square = S.S/D.F.

$$0.44V + 0.19F - 1.76S + 2.11N + 1.43V^2 + 1.22S^2 + 0.62N^2 - 0.94FS + 0.77FN \quad (12)$$

$$\text{Percentage of dilution} = 47.27 + 0.74V + 2.51F - 0.25S - 2.25N - 1.3V^2 - 0.7F^2 - 1.31S^2 - 0.45N^2 - 0.9FN \quad (13)$$

$$\text{Total weld bead volume, mm}^3 = 46.06 + 1.58V + 2.2F - 3.5S + 2.0N + 1.66V^2 + 1.35S^2\ 0.95N^2 - 0.87FS \quad (14)$$

where V = welding voltage, F = wire feed rate, S = welding speed and N = nozzle-to-plate distance.

**Conducting the Conformity Tests**

To determine the accuracy of the mathematical models developed, conformity test runs were conducted with the same experimental setup. The conformity tests were conducted about two years after the mathematical models were developed. In the conformity test runs, the process variables were assigned some intermediate values, and the responses were measured. A comparison was made between the actual and predicted values of bead parameters, and the results are given in Table 6. The results show the accuracy of the models developed was above 97%.

## Results and Discussions

The mathematical models furnished above can be used to predict the weld bead geometry by substituting the values of the respective process parameters. Also, the values of the control factors can be obtained by substituting the value of the desired bead geometry. The responses calculated from the reduced models for each set of coded values of welding variables are represented graphically in Figs. 2–18; these show generally convincing trends between cause and effect.

**Direct Effects of Parameters**

The Direct Effect of Welding Voltage (V) on Bead Parameters

Figure 2 shows the penetration (P) and reinforcement (R) decrease marginally but the bead width (W) and the percentage of dilution (D) increase steadily with the increase in welding voltage (V). The increase in V results in increased arc length, which results in more melting at the surface; hence, P decreases. Also, the increase in the arc length results in spreading of the arc cone. Hence, W increases considerably as V increases. As the rate of decrease in P is less than W's rate of increase with an increase in V, the weld pool size increases and, hence, D increases. The increased voltage resulted in increased bead width with corresponding reduction in reinforcement height (R) due to the spreading of the base of the arc cone. An excessive increase in voltage can result in nearly flat bead. Hence, R as well as the area of excess metal deposited on the base plate decrease as V increases.

Jackson (Ref. 16) reported about the relationship between penetration and welding voltage and current and welding speed using a welding technique performance factor, given as

$$\sqrt[3]{I^4/SE^2}$$

where I = welding current (amps), S =

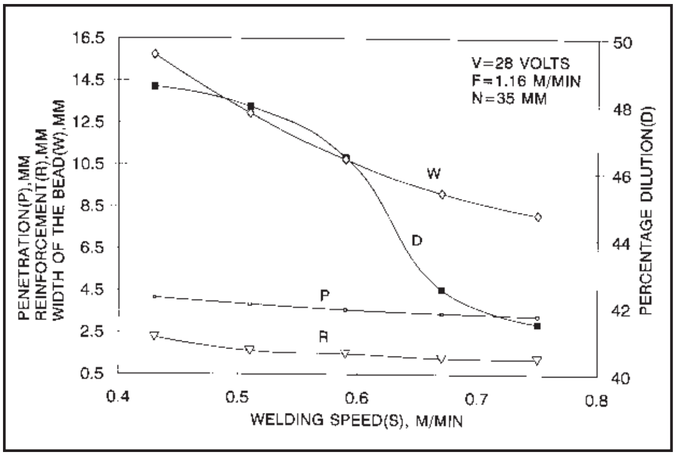


*Fig. 7 — Direct effect of welding speed (S) on bead parameters P, R, W and D.*

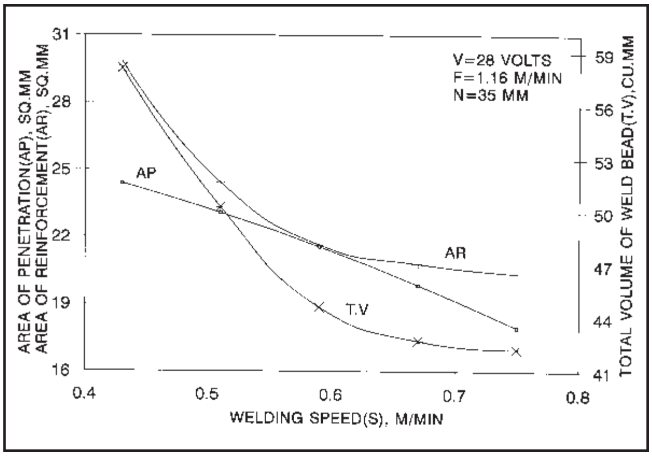


*Fig. 8 — Direct effect of welding speed (S) on bead parameters AP, AR and T.V.*

welding speed, (m/min [in. / min]) and E = welding voltage (in volts).

The welding technique performance factor related to penetration, shown in Fig. 3, is found to have the same trend as reported. In the figure, note P tends to increase with the increase of the welding performance factor.

Figure 4 shows the area of penetration (AP) increases but both area of reinforcement (AR) and total volume of weld bead (T.V) decrease to an optimum value as V increases from 24 to 28 volts; then AR and T.V increase for a further increase in V. As V increases, P decreases slightly, but W increases steadily, as shown in Fig. 2. Weld pool size increases, resulting in an increase of AP. But R decreases gradually as V increases from 24 to 28 volts, and, for further increase in the value of V, R is almost constant whereas W increases steadily. Also, when V is increased from 24 to 28 volts, the rates of decrease in R and, thus, AR are more than the rate of increase in AP. Hence, T.V decreases as V is increased up to 28 volts and, with a further increase in V, results in a steady increase in T.V.

**Table 5 — Comparison of Squared Multiple R Values and Standard Error of Estimate Values for Full and Reduced Mathematical Models**

| S. No. | Bead Parameters | $R^2$ Value (adjusted) Full models | $R^2$ Value (adjusted) Reduced models | Standard error of estimate Full models | Standard error of estimate Reduced models |
|---|---|---|---|---|---|
| 1 | Penetration | 0.598 | 0.700 | 0.280 | 0.242 |
| 2 | Reinforcement | 0.777 | 0.819 | 0.144 | 0.130 |
| 3 | Bead width | 0.941 | 0.943 | 0.546 | 0.533 |
| 4 | Area of penetration | 0.850 | 0.878 | 0.984 | 0.887 |
| 5 | Area of reinforcement | 0.748 | 0.774 | 1.762 | 1.671 |
| 6 | Percent dilution | 0.869 | 0.880 | 1.379 | 1.317 |
| 7 | Total weld bead volume | 0.786 | 0.808 | 2.437 | 2.312 |

The Direct Effect of Wire Feed Rate (F) on Bead Parameters

Figures 5 and 6 show all the important bead parameters — P, R, W, D, AP, AR and T.V — increase with the increase in F. This is because the arc current and, hence, the heat input increase with the increase in F, and the wire melting and deposition rate increase as F increases. Therefore, because of high heat input and metal deposition rate, P, R, W, D, AP, AR and T.V all increase when F increases.

The Direct Effect of Welding Speed (S) on Bead Parameters

From Figs. 7 and 8, it is apparent the welding speed (S) has a negative effect on all the bead parameters. This is because, when S increases, the welding torch travels at a greater speed over the base metal, resulting in a lower metal deposition rate on the joint. Also, the heat input decreases appreciably when S increases. Hence, because of less heat input and a lower metal deposition rate, P, R, W, D, AP, AR and T.V all decrease with the increase in the value of S.

The Direct Effect of Nozzle-to-Plate Distance (N) on Bead Parameters

Figure 9 shows that as the nozzle-to-plate distance (N) increases, R and D decrease, but the reverse is true with W. These effects occur because the arc current and, hence, the heat input decrease with the increase in N. Because of the reduced heat input, the value of R and D decrease when N increases. As N increases, the arc length increases. This increase in the arc length spreads the arc cone at its base. Also, the metal fusion rate increases slightly at higher values of N because of the joules heating effect. Therefore, the value of W increases as N increases. P is not significantly affected by N.

Figure 10 shows AP decreases slightly but AR and T.V increase steadily with the increase in N. As N increases, P decreases very little and, hence, AP decreases. The decrease in R (from 1.31 to 1.27 mm ) is much lower compared to the increase in W (from 11 to 12 mm) when N is increased, as shown in Fig. 9. Hence, AR increases appreciably with the increase in N. Also, the increase in AR is steady compared to the decrease in AP as N increases. Therefore, the total area and T.V of the weld bead increase steadily with the increase in N.

**Interaction Effects of Process Variables**

Interaction Effects of Wire Feed Rate (F) and Welding Speed (S) on Bead Width (W)

Figure 11 shows the interaction effect of F and S on W. From the direct effects of F and S (shown in Figs. 5 and 6) on W, it was found F has a positive effect but S has a negative effect on W. Because of these effects, the value of W increases with the increase in F for all values of S. But, because of the negative effect of S on W, the rate of increase W with the increase in F gradually decreases as S increases from its lower limit to upper limit.

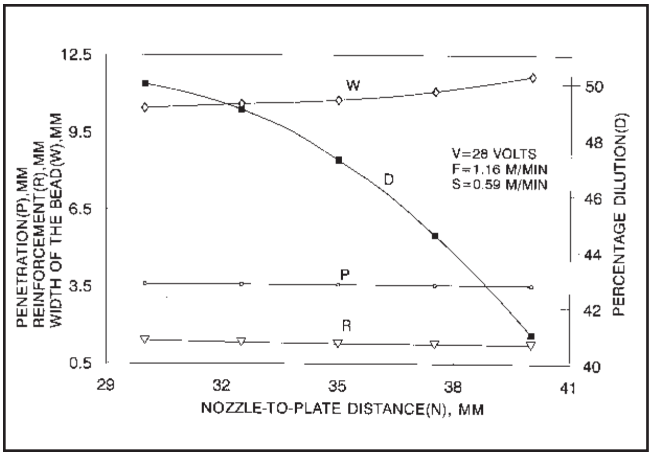


*Fig. 9 — Direct effect of nozzle-to-plate distance (N) on bead parameters P, R, W and D.*

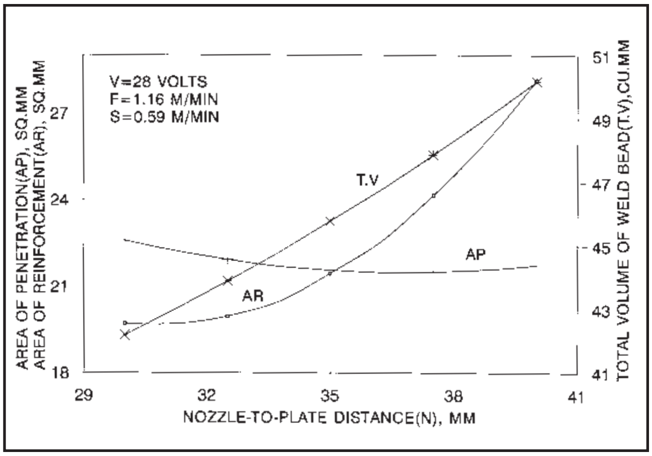


*Fig. 10 — Direct effect of nozzle-to-plate distance (N) on bead parameters AP, AR and T.V.*

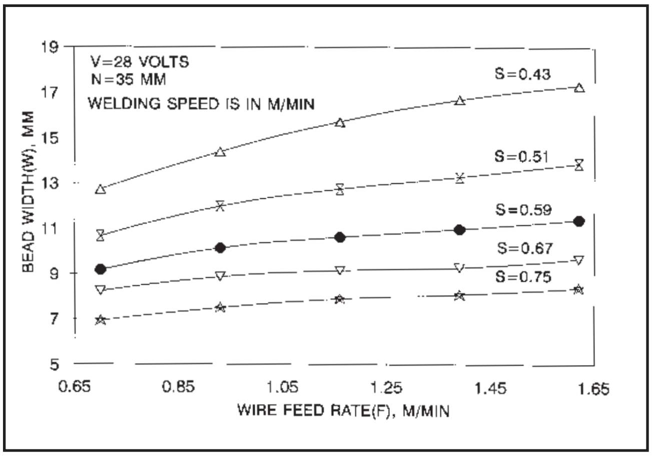


*Fig. 11 — Interaction effect of F and S on bead width.*

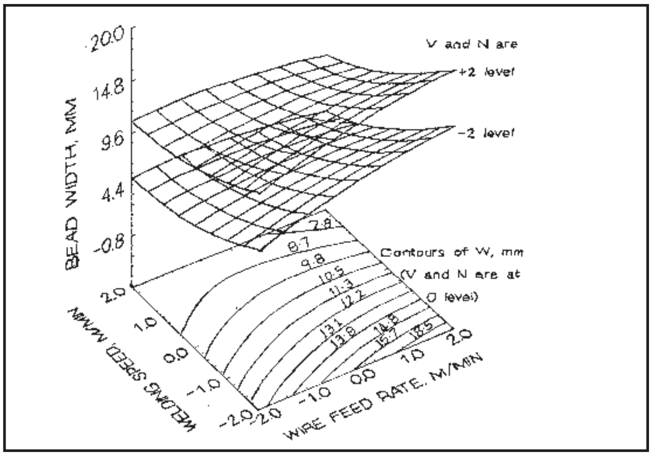


*Fig. 12 — Interaction effect of F and S on bead width (response surface).*

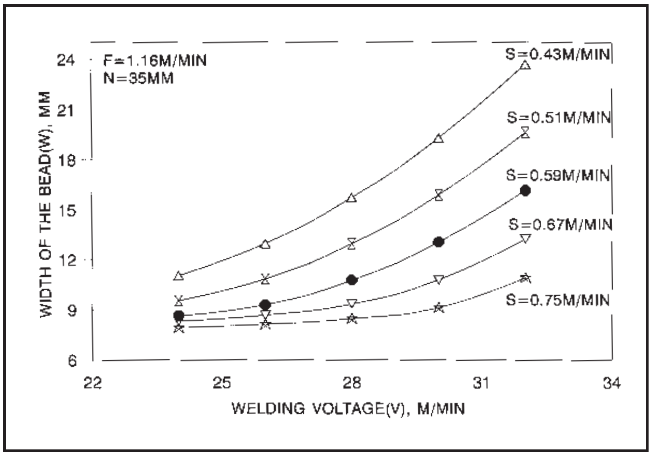


*Fig. 13 — Interaction effect of V and S on bead width.*

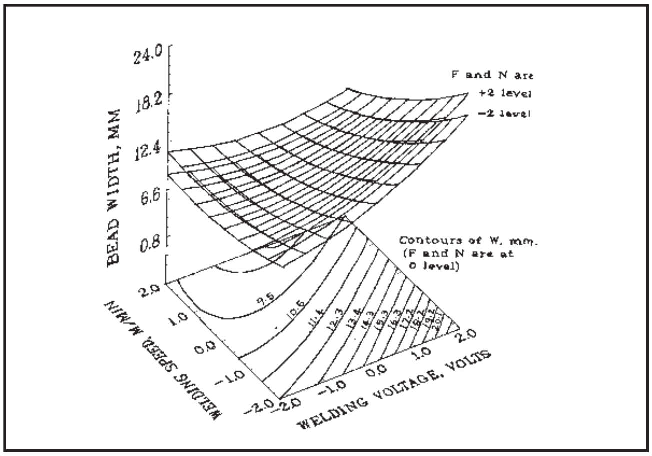


*Fig. 14 — Interaction effect of V and S on bead width (response surface).*

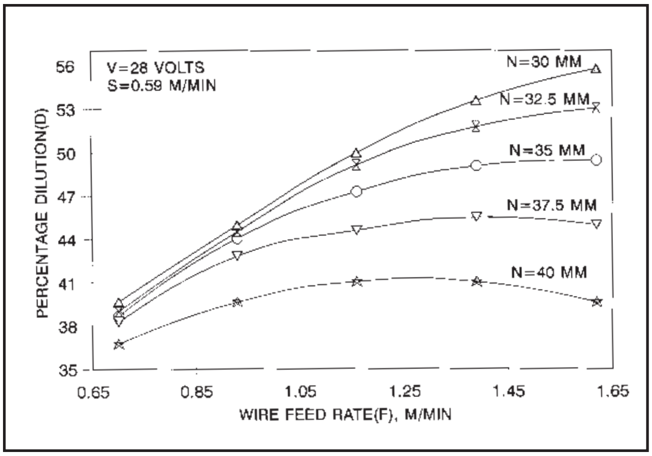


Fig. 15 — Interaction effect of F and N on bead dilution.

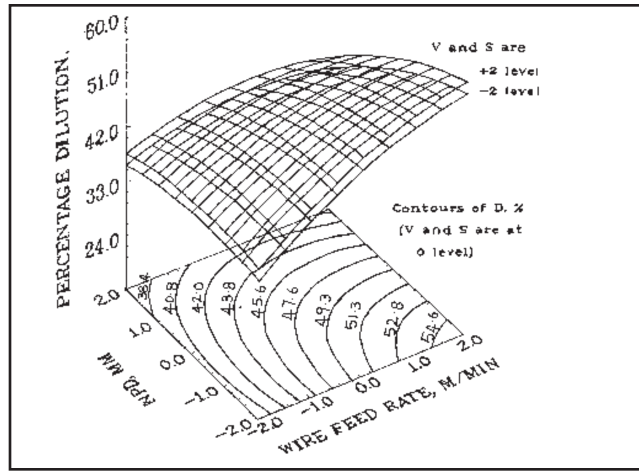


Fig. 16 — Interaction effect of F and N on bead dilution (response surface).

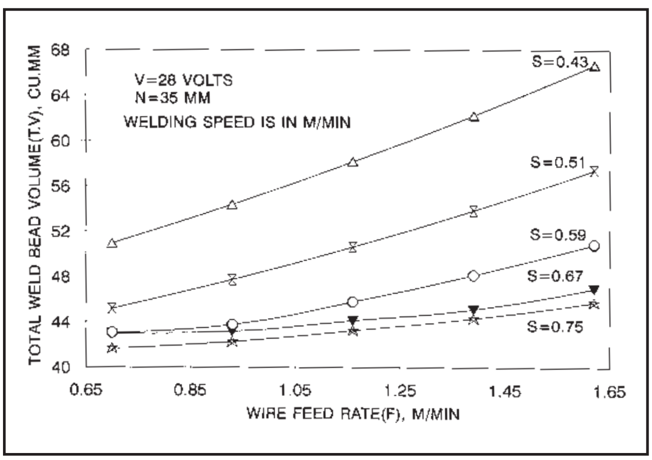


Fig. 17 — Interaction effect of F and S on total weld bead volume.

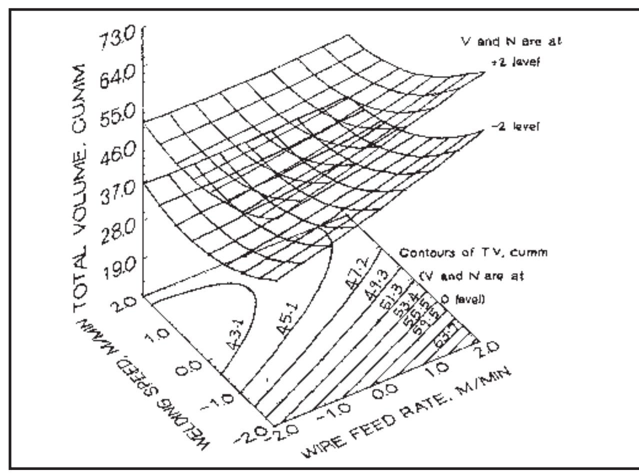


Fig. 18 — Interaction effect of F and S on total weld bead volume (response surface).

Figure 12 shows the response surface and the contour plot of W for the interaction of F and S when V and N are kept at zero (0). From this contour surface, it is found W is lowest (8 mm) when F is at its minimum value with S at its maximum value; W is highest (17 mm) when F is at its maximum value with S at its minimum value.

Interaction Effect of Welding Voltage (V) and Welding Speed (S) on Bead Width (W)

From Fig. 13, it is evident W increases as V increases for all values of S. But this increasing trend of W with the increase in V decreases gradually as S increases. These effects occur because V has a positive effect but S has negative effect on W, as shown in Figs. 2 and 7. At the lowest value of V, W is maximum (11 mm) for the lower value of S (0.43), and W is minimum (8 mm) for the higher value of S (0.75). Also, when V is at its maximum value, W is maximum (24 mm) for the lower value of S and is minimum (11 mm) for the higher value of S. These effects are further explained in Fig. 14, which shows the contour plot of W for the interaction effect of V and S when F and N are at their midpoints (0). From the contour surface of W, it is observed W is maximum (about 20 mm) when V is at its upper level (+2) with S at its lower level (–2); W is minimum (about 9 mm) when V is at its lower level (–2) with S at its upper level (+2).

Interaction Effect of Wire Feed Rate (F) and Nozzle-to-Plate Distance (N) on Bead Dilution (D)

Figure 15 shows the interaction effect of F and N on D. From the direct effects of F and N on D (as discussed previously and shown in Figs. 5 and 9), it was found F has a positive effect but N has a negative effect on D. Because of these effects, and their interaction effect on D shown in Fig. 15, the value of D increases steadily with the increase in F for all values of N. But this rate of increase in D with increase in F gradually decreases as N increases from 30 to 40 mm.

Figure 16 shows the response surface of D for the interaction effect of F and N. The contour surface shows D is maximum (54.6%) when F is at its maximum limit (+2) with S at its minimum limit (–2), and D is minimum (36.4%) when F is at its lower level (–2) with N at its upper level (+2).

Interaction Effect of Wire Feed Rate (F) and Welding Speed (S) on Total Weld Bead Volume (T.V)

Figure 17 shows T.V increases steadily with the increase in F for any given value of S. But this increase of T.V with the increase in F decreases gradually as S increases from its lower value (0.43) to its upper value (0.75). These effects are mainly due to the positive effect of F but negative effect of S on T.V (as explained previously and shown in Figs. 6 and 8).

Figure18 shows the response surface of T.V due to the interaction effects of F and S. The contour graph also shows the same trend for T.V. This graph shows T.V is maximum (64.2 $mm^3$) when F is at its maximum value with S at its minimum limit. T.V is minimum (42.5 $mm^3$) when F is at its lower value with S at its upper limit.

## Conclusions

The following conclusions were drawn from the above investigation:

1) The five-level factorial technique can be employed easily for developing mathematical models for predicting weld bead geometry within the workable region of process parameters for SAW of pipes.

2) The models developed can be employed easily in the form of a program for automatic and robotic welding for obtaining the desired high-quality welds.

3) The welding process variable wire feed rate has a positive effect, but welding speed has a negative effect on all the bead parameters.

4) Penetration reduces as welding voltage increases, but bead width and dilution increase considerably with the increase in voltage.

5) Reinforcement is least when all the process variables are at their upper limit (+2) and F is at its lower limit.

6) Nozzle-to-plate distance has a negative effect on all the bead parameters except bead width and total volume of the weld bead.

7) Most of the direct and interaction effects of the process variables on the bead parameters show generally convincing trends between cause and effect.

*References*


1. Houldcroft, P. T. 1989. *Submerged Arc Welding*. Abington Publishers, U.K.

2. Annon. 1978. *Principles of Industrial Welding.* The James F. Lincoln Arc Welding Foundation, Cleveland, Ohio.

3. Balckman, S. 1981. Welded fabrication of subsea pipelines in the north sea. *Welding and Metal Fabrication.*

4. Murugan, N., Paramar, R. S., and Sud, S. K. 1993. Effect of submerged arc process variables on dilution and bead geometry in single wire surfacing. *Journal of Materials Processing Technology* 37: 767–780.

5. Adler, Y. P., Markov, E. V., and Granovsky, Y. V. 1975. *The Design of Experiments to Find Optimal Conditions*. MIR Publishers, Moskow.

6. Fisher, R. A. 1952. *Statistical Methods for Research Workers,* 12th edition. Edinburgh, Oliver and Boyd.

7. Gupta, V. K., and Parmar, R. S. 1986. Fractional factorial techniques to predict dimensions of the weld bead in automatic submerged arc welding. *Journal of Inst. of Engineers* (India) 70:67–71.

8. Arya, S. K., and Parmar, R. S. 1986. Mathematical models for predicting angular distortion in $CO_2$ — shielded flux cored arc welding. *Proceedings of the International Conference on Joining of Metals*, pp. 240–245.

9. Murugan, N., and Parmar, R. S. 1994. Effects of MIG process parameters on the surfacing of stainless steel. *Journal of Materials Processing Technology* 41: 381–398.

10. Cochran, W. G., and Cox, G. M. 1963. *Experimental Designs.* Asia Publishing House, India.

11. Khuri, A. I., and Cornell, J. A. 1996. *Response Surfaces, Design and Analysis.* Marcol Dikker Inc., New York, N.Y.

12. Box, G. E. P., and Voule, P. V. 1955. The exploration and exploitation of response surfaces. *Biometrics* 11:287–322.

13. Montgomery, D. C., and Peck, E. A. 1992. *Introduction to Linear Regression Analysis.* John Wiley, New York, N.Y.

14. Davis, O. L. 1978. *The Design and Analysis of Industrial Experiments.* Longman, New York, N.Y.

15. SYSTAT Version 5.02. 1991. Systat, Inc.

16. Jackson, C. E, and Shrubsall, A. E. 1953. Control of penetration and melting ratio with welding technique. *Welding Journal*: 32(4): 172-s to 178-s.